Nanoscale Advances

ROYAL SOCIETY OF CHEMISTRY

MINIREVIEW

View Article Online
View Journal | View Issue

Cite this: *Nanoscale Adv.*, 2022, **4**, 1060

Nanoscale interface engineering for solid oxide fuel cells using atomic layer deposition

Jongsu Seo,†[a] Seunghyun Kim,†[a] SungHyun Jeon,[a] Suyeon Kim,[b] Jeong Hwan Kim*[b] and WooChul Jung*[a]

Received 6th December 2021
Accepted 9th January 2022

DOI: 10.1039/d1na00852h

rsc.li/nanoscale-advances

Atomic layer deposition (ALD), which is already actively used in the semiconductor industry, has been in the spotlight in various energy fields, such as batteries and fuel cells, given its unique ability to enable the nanoscale deposition of diverse materials with a variety of compositions onto complex 3D structures. In particular, with regard to ceramic fuel cells, ALD has attracted attention because it facilitates the manufacturing of thin and dense electrolytes. Furthermore, recently, electrode surfaces and electrode/electrolyte interface modification are arising as new research strategies to fabricate robust fuel cells. In this mini-review, we present a brief overview of ALD and recent studies that utilize ALD in ceramic fuel cells, such as manufacturing thin film electrolytes, stabilizing electrodes, functionalizing electrodes, and modifying the chemistry of electrode surfaces. We also propose research directions to expand the utility and functionality of the ALD techniques.

Introduction

The global increases in energy demand and environmental problems have made it increasingly important to develop highly efficient and environmentally friendly power generation technologies. Among them, the solid oxide fuel cell (SOFC) is attracting much attention as a future power generation device due to its advantages of high energy efficiency and fuel flexibility compared to other fuel cells.[1–3] In addition, these fuel cells are suitable for a distributed generation due to their small installation area, and they can be utilized as a combined heat and power system by not only supplying electricity to buildings but also converting heat to hot water/heating systems, maximizing the overall system efficiency.[1] However, their high operating temperatures, typically exceeding 800 °C, thermal management issues, limited material selection, and degradation issues leading to increased device costs, all act as obstacles preventing their full-scale commercialization.[4,5]

In order to solve these problems fundamentally, studies are being actively conducted to operate SOFCs at an intermediate temperature of 700 °C or lower. However, lowering the operating temperature can cause higher ohmic losses of the electrolytes and a rapid decrease in the electrode activity, which results in low energy conversion efficiency.[6,7] Therefore, to realize high-performance SOFCs at intermediate temperatures,

[a]*Department of Materials Science and Engineering, Korea Advanced Institute of Science and Technology (KAIST), Daejeon, Republic of Korea. E-mail: wcjung@kaist.ac.kr*

[b]*Department of Materials Science and Engineering, Hanbat National University, Daejeon, Republic of Korea. E-mail: jkim@hanbat.ac.kr*

† These authors contributed equally to this work.

Jongsu Seo received his PhD from the Department of Materials Science and Engineering, Korea Advanced Institute of Science and Technology (KAIST) in 2021. Currently, he is a post-doctoral fellow in the same institute. His research interests focus on nanocatalysts, metal–oxide interfaces, atomic layer deposition and related energy devices such as solid oxide fuel cells.

Seunghyun Kim received her master's degree from the Department of Materials Science and Engineering, Korea Advanced Institute of Science and Technology (KAIST) in 2019. Currently, she is a PhD candidate in the same institute. Her research interests focus on supported metal nanocatalysts, metal–oxide interfaces and related energy devices.

reducing the ohmic loss and developing highly active/robust electrodes must come first. In an effort to reduce the ohmic loss of the electrolyte, a thin film electrolyte fabrication process is being developed along with studies of new material compositions for ion conductors.[8,9] Meanwhile, in order to develop high-performance SOFC electrodes that function at intermediate temperatures, numerous studies to control the microstructures of the electrode and to functionalize the electrode surfaces through nanoscale surface engineering are being conducted.[10]

From this point of view, atomic layer deposition (ALD) represents a technology capable of fabricating dense oxide thin films, and it has the best step coverage among existing deposition techniques, enabling uniform and sophisticated coatings onto complicated structures.[11,12] ALD is already a commercial technology utilized in the production lines of the semiconductor industry to achieve maximum productivity through nanoscale engineering. Moreover, due to its advantage of being able to coat metals and oxides with various compositions at a low temperature, ALD is widely applied in the sensor, battery, fuel cell fields, all of which require elaborate nanoscale processes.[13–17] In fact, the number of review articles dealing with the energy and catalysts field such as fuel cells, battery, heterogeneous catalysts, water splitting, *etc.* with "ALD" as a keyword has increased by 68% within the past five years, proving the importance of the application of ALD in energy-related fields (Fig. 1). Among these, eight review papers focused on applications to SOFCs, indicating that ALD is also being actively utilized in relation to these fuel cells.

In this review, we focus on reports that introduce ALD to realize high-performance SOFCs within the last three years. Although ALD is not yet heavily used in the manufacturing process of SOFC cells or stacks, recent studies have reported that it can improve SOFC performance outcomes by creating a new functional interlayer between the electrode and electrolyte composed of ceramic materials. Here, we are going to cover from the brief ALD overview, of which properties lead to the successful application of ALD to the SOFC electrode research, to studies using ALD for electrolytes, electrode/electrolyte interface reforming, suppressing degradation, and introducing metal/oxide composite catalyst. Through this, we will examine the significant contribution of ALD in the field of SOFC and suggest the direction for the future advance of ALD technology for the development of the SOFC field.

SungHyun Jeon received his master's degree from the Department of Materials Science and Engineering, Korea Advanced Institute of Science and Technology (KAIST), Korea, and is currently pursuing for a PhD degree in the same institute. His research interests focus on nanocatalysts, atomic layer deposition, and related energy devices such as solid oxide fuel cells.

Jeong Hwan Kim received his BS and PhD degree from Seoul National University, Seoul, South Korea, in 2011. He is now an Assistant Professor with the Department of Materials Science and Engineering at Hanbat National University, Daejeon, South Korea. His current research interests are focused on functional thin-film materials and coating technology on nanostructured surfaces using atomic layer deposition (ALD) and physical vapor deposition (PVD) processes for energy devices and flexible electronics applications.

Suyeon Kim received her BS degree from the Department of Materials Science and Engineering, Hanbat National University, Daejeon, in 2021. Currently, she is a MS candidate in Hanbat National University. Her research interests focus on thin films deposition and nanomaterials.

WooChul Jung received his PhD in Materials Science and Engineering from MIT and served as postdoctoral fellow in Materials Science at Caltech. He is now an associate professor of the department of MSE at Korea Advanced Institute of Science and Technology (KAIST). His research interests focus on the characterization and optimization of interface reaction kinetics between gases and ionic solids for applications in solid oxide fuel cells, electrolyzers and gas permeation membranes.

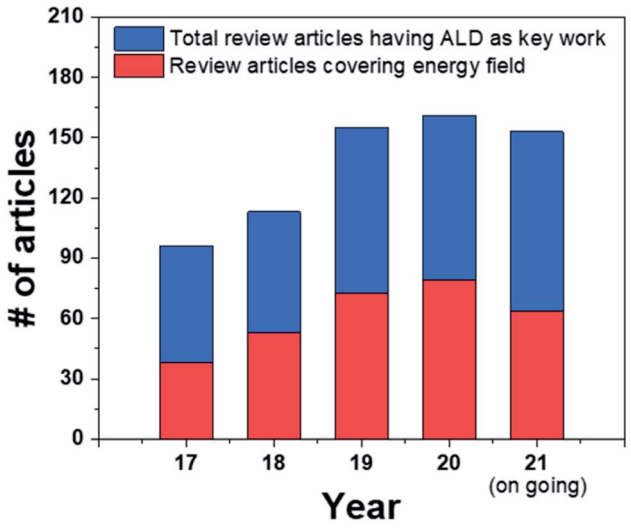

Fig. 1 The number of review articles relevant with the ALD from 2017 to todays.

A brief overview of atomic layer deposition

Since atomic layer deposition (ALD) was first proposed by a research team at the University of Helsinki, Finland in 1970, it has been developed into a fabrication technique for high-quality dielectric films in the semiconductor field. This technique has achieved atomic-level controllability of film thickness and chemical composition along with excellent step coverage.[11,12] In the ALD process, a thin film forms by repeated cycles of supply and purging of precursors and reactants, which are separately and sequentially supplied to the substrate surface (Fig. 2). Therefore, unlike other vacuum-based deposition techniques, ALD exhibits the following characteristics.

The most representative characteristic is the self-limiting reaction, which pertains to the growth saturation behavior of the chemisorbed molecules with all reactive sites on the surface. The excessively supplied precursors and reactant molecules, which are physisorbed on the chemisorbed molecules, are removed during the purging step, resulting in a sole monolayer growth within an ALD cycle.[18,19] This self-limiting characteristic allows excellent thickness uniformity and step-coverage. The second characteristic is the linearity of the as-grown thin film thickness as a function of the number of ALD cycles; this is due to the monolayer growth in each of the ALD process cycles and the thin film growth by the monolayer stacking mechanism through cycle repetition.[20,21] Consequently, ALD allows for precise thickness control at the angstrom level through cycle count control. Lastly, the ALD growth rate in a specific temperature range is insensitive to the deposition temperature, which is a very important process variable for chemical vapor deposition (CVD). There is a temperature range called the ALD temperature window wherein the film growth rate is constant.[22] This then enables consistent thin film deposition over a large-area substrate, even that with temperature sensitivity, which is important for mass production.[23]

With these characteristics, ALD even allows the surface engineering of structures with high-aspect ratio at the nano-level, which cannot be realized by other vacuum-based deposition techniques.[24,25] In addition, by controlling the number of sub-cycles for each precursor constituting the super-cycle, as shown in Fig. 3, one can precisely vary the chemical composition of the coating layer.[26–28] Therefore, ALD has been

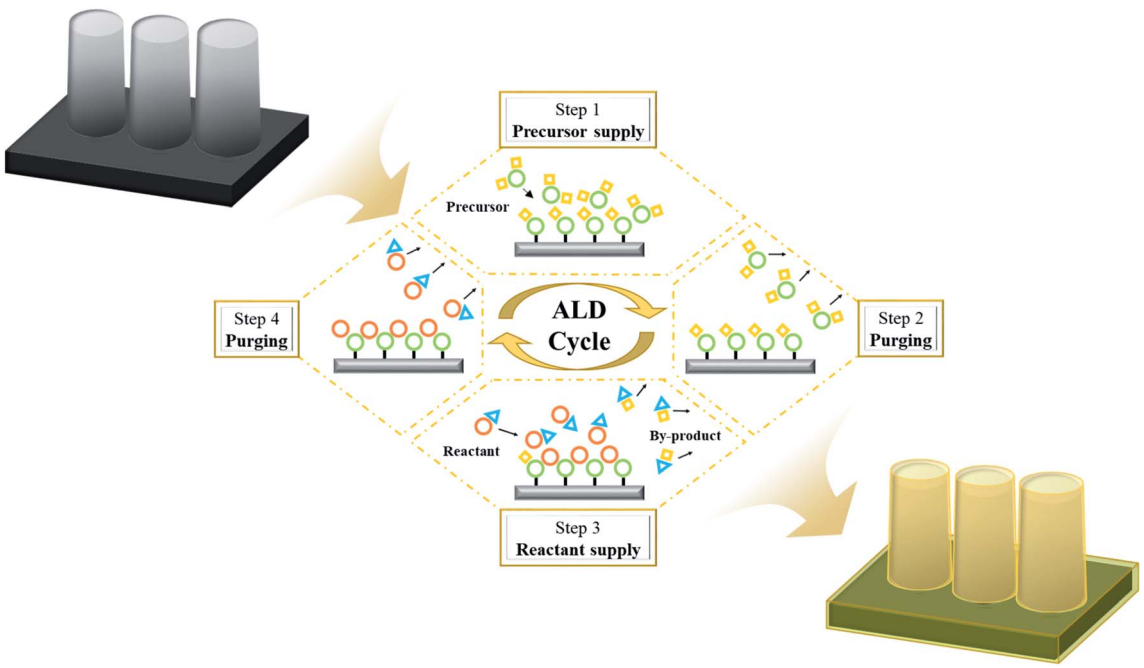

Fig. 2 Schematic representation of the surface engineering by ALD on high aspect ratio structures.

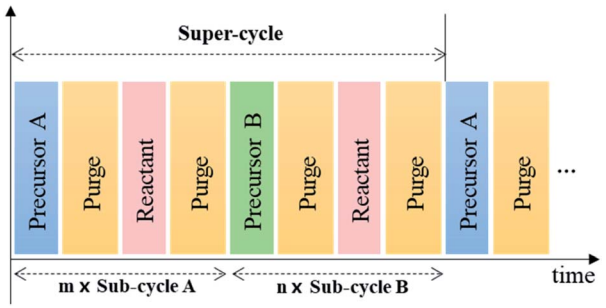

Fig. 3 Schematic diagram of ALD super-cycle for varying the chemical composition.

successfully applied not only to displays and semiconductors but also to various energy devices that require nanoscale surface engineerings such as solar cells, batteries, sensors, and fuel cells.[14,15,17,29,30]

ALD for thin film electrolytes

Thin and dense electrolyte fabrication is crucial for the development of high-performance SOFCs. Many processes that minimize the ohmic loss and gas leakage of the electrolyte have been suggested to prepare dense thin films.[8,31–33] Compared to conventional methods such as the sol–gel or sputtering approaches, the ALD process can ensure a dense structure without gas leakage, even with very thin thicknesses, and this can contribute to the enhanced power density of a SOFC.[34–37] As shown in Fig. 4a, Prinz *et al.* fabricated yttria-stabilized zirconia (YSZ), a commonly used material for SOFC electrolytes, through ALD and reported its properties.[37] A microstructural analysis shows a dense and uniform layer of YSZ electrolyte deposited between sputtered Pt electrodes. When comparing the power density of the cells at 350 °C with 50 nm-thick YSZ electrolyte fabricated by RF-sputtering and ALD, it was confirmed that the power density of the cell using ALD showed twice the level of enhancement (Fig. 4b). The research team reported that the performance enhancement was due to the slightly better ion conductivity property of the electrolyte fabricated by ALD compared to the RF-sputtered sample. Moreover, the YSZ electrolyte deposited by ALD has nano-sized grains, and the outstanding oxygen exchange rate also contributed to the considerable enhancement in the electrode activity.

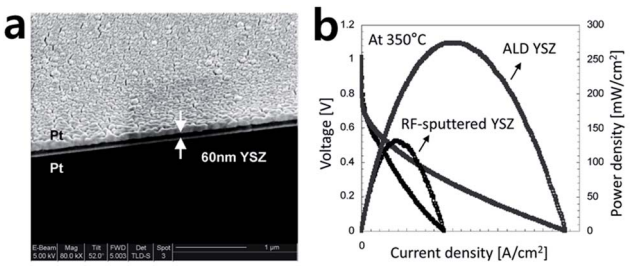

Fig. 4 (a) SEM image of ALD YSZ film between porous Pt cathode and anode. (b) Performance comparison of ALD YSZ fuel cells to fuel cells with 50 nm RF-sputtered YSZ. Figures reproduced with permission from ref. 37. Copyright 2007, American Chemical Society.

Recently, An *et al.* proposed a sandwich-structured thin film composite electrolyte fabricated by ALD (Fig. 5a).[36] Doped cerium oxide is considered as an excellent electrolyte material due to its high electrode activity at the triple-phase boundary (TPB) and has high ion conductivity compared to YSZ. However, aside from its high ion conductivity, it also has low electron conductivity, which triggers leakage current and thus lowers the overall energy efficiency of the SOFC system. To overcome this issue, a sandwich structure that involved inserting a very thin YSZ layer *via* ALD between samaria-doped ceria (SDC) electrolytes was proposed, blocking the leakage current with a trivial effect on the total ohmic loss and achieving around six times the performance of a sample for which only one side of the SDC was coated by YSZ (Fig. 5b).

Along with attempts to realize thin film electrolyte fabrication, studies to investigate optimal electrolyte material compositions by controlling the number of ALD cycles are ongoing. YSZ is traditionally known to have optimal ion conductivity with 8 mol% of yttrium. Cha *et al.* prepared YSZ thin films with various compositions (32.1 mol%, 19.5 mol%, 14.0 mol%, 10.7 mol%, 7.2 mol%, and 4.9 mol%) by controlling the number of ALD cycles for ZrO_2 and Y_2O_3 (Fig. 5c).[34] In their case heavily doped 10.7 mol% YSZ showed the highest peak power density at 450 °C. This result of 180 mW cm^{-2} represents a nearly 26% enhancement in the peak power density compared to 8 mol% YSZ, previously considered to have the highest ionic conductivity (Fig. 5d). The authors argue that heavily doped Y leads to an increase in the number of oxygen vacancies available on the TPB, promoting the oxygen reduction reaction (ORR) and hydrogen oxidation reaction (HOR) activities and resulting in high performance. On the other hand, with low Y doping, not enough oxygen vacancies could be generated, and with excessive Y doping, oxygen vacancies agglomerate, resulting in lower performance. This result has implications because not only the fabrication of the thin electrolyte but also the material optimization could be realized by precisely controlling the composition through ALD. In the same manner, studies aiming to enhance SOFC performance outcomes by improving the electrode–electrolyte interface property by inserting a very thin inter-layer with various compositions between the electrode and electrolyte are ongoing.[38–40] Recently, Kim *et al.* deposited various compositions of gadolinia-doped ceria (GDC, Gd_2O_3 doping ratio: 11.9 mol%, 13.9 mol%, 18.8 mol%, and 25.2 mol%) onto the interface of YSZ and a Pt electrode and measured the peak power density (Fig. 5e).[39] The optimal performance was achieved when 18.8 mol% of Gd-doped ceria was inserted as an inter-layer, and power density of 288.24 mW cm^{-2} was obtained with three times greater performance at 450 °C (Fig. 5f). As such, studies that concentrate on the characterization and optimization of various new material compositions by precisely adjusting the concentrations by controlling the ALD cycle are being conducted.

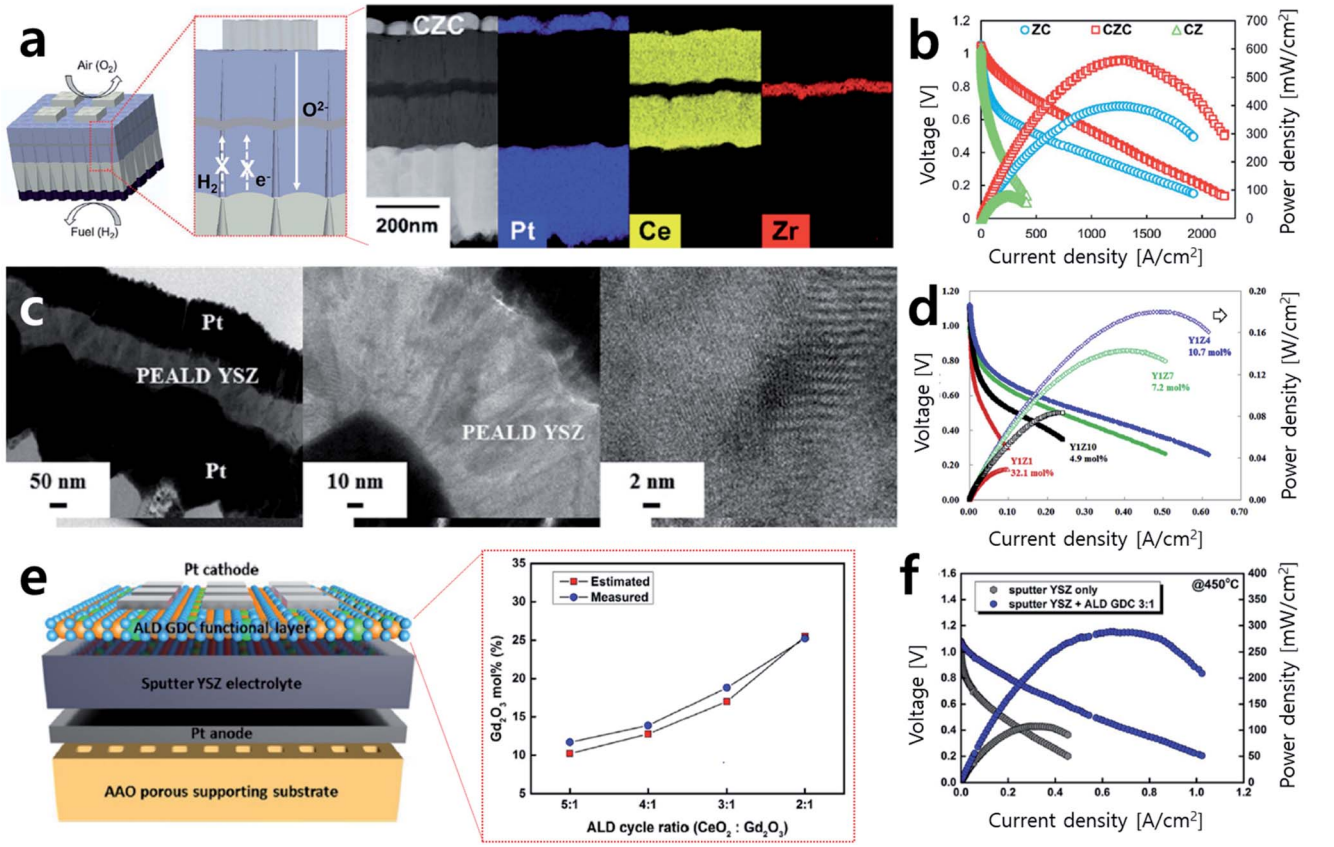

Fig. 5 (a) Schematics of sandwich-structured SOFCs and cross-sectional TEM images and EDS mapping of prepared sandwich SOFCs. (b) Performance comparison of sandwich-structured cells (CZC) to cells with single side coated electrolyte (CZ, ZC). (c) Cross-sectional TEM images of cells with 10.7 mol% ZrO_2 doped Y_2O_3 electrolyte prepared by ALD and its magnified images of the electrolyte. (d) Performance comparison of cells according to the concentration of ZrO_2 doping level. (e) Schematics of GDC functional layer and the atomic ratio of Gd_2O_3 in GDC depending on ALD cycle ratio. (f) Current–voltage (I–V) curves and power density of cells with and without an ALD functional layer. Figures reproduced with permission from ref. 34, 36 and 37. Copyright 2018, The Royal Society of Chemistry, Copyright 2019, Elsevier, and Copyright 2021, Wiley.

ALD for electrodes

In addition to the advantage of accurately controlling the composition of the thin film and depositing dense thin films with nanosized grains, the ALD process is capable of uniformly coating complex structures due to its excellent step coverage. ALD can stabilize and/or functionalize the surfaces or interfaces of SOFC electrodes by uniformly coating complex 3D structures. In this chapter, three categories of examples of ALD contributing to SOFC electrode studies will be introduced: (1) overcoming the thermal and chemical degradation at high temperatures through an ALD coating, (2) functionalizing electrode surfaces with a coating of a functional oxide or by introducing metal catalysts, and (3) tailoring oxides surface to facilitate the self-assembly of nanocatalysts.

Studies of the thermal/chemical stabilization of electrodes

Precious metals or transition metals such as Pt, Ag, Ni, and Ru are often used as SOFC electrode materials due to their high conductivity as well as their superior catalytic activity towards the ORR on the cathode side and the fuel oxidation reaction on the anode side.[31–50] However, due to their high operation temperatures, electrode materials can become agglomerated, resulting in an interruption of the electron flow and decreases in the electrode surface area and triple-phase boundary (TPB), known as the major reaction sites.[44] These phenomena cause irreversible performance degradation. Therefore, dealing with this issue is essential for the long-term operation of SOFCs. To resolve this, many attempts have been made to improve the thermal stability of metal electrodes by various oxide coatings.[42–44,46,48–51]

As an example, Jung *et al.* adopted an Al_2O_3 coating by ALD successfully to stabilize a porous Pt electrode, which tends to undergo microstructural agglomeration within only ten hours of exposure at 500 °C (Fig. 6a).[48] A relatively thick Al_2O_3 coating of 6 nm could stabilize the electrode, but the activity was reduced due to the overly thick deposition of an insulator of Al_2O_3. Nevertheless, an appropriate thickness of 3.6 nm Al_2O_3 coated onto a Pt electrode could maintain its initial microstructure and even show two times higher electrode performance compared to an uncoated sample. This study is meaningful because not only was the stability of the metal

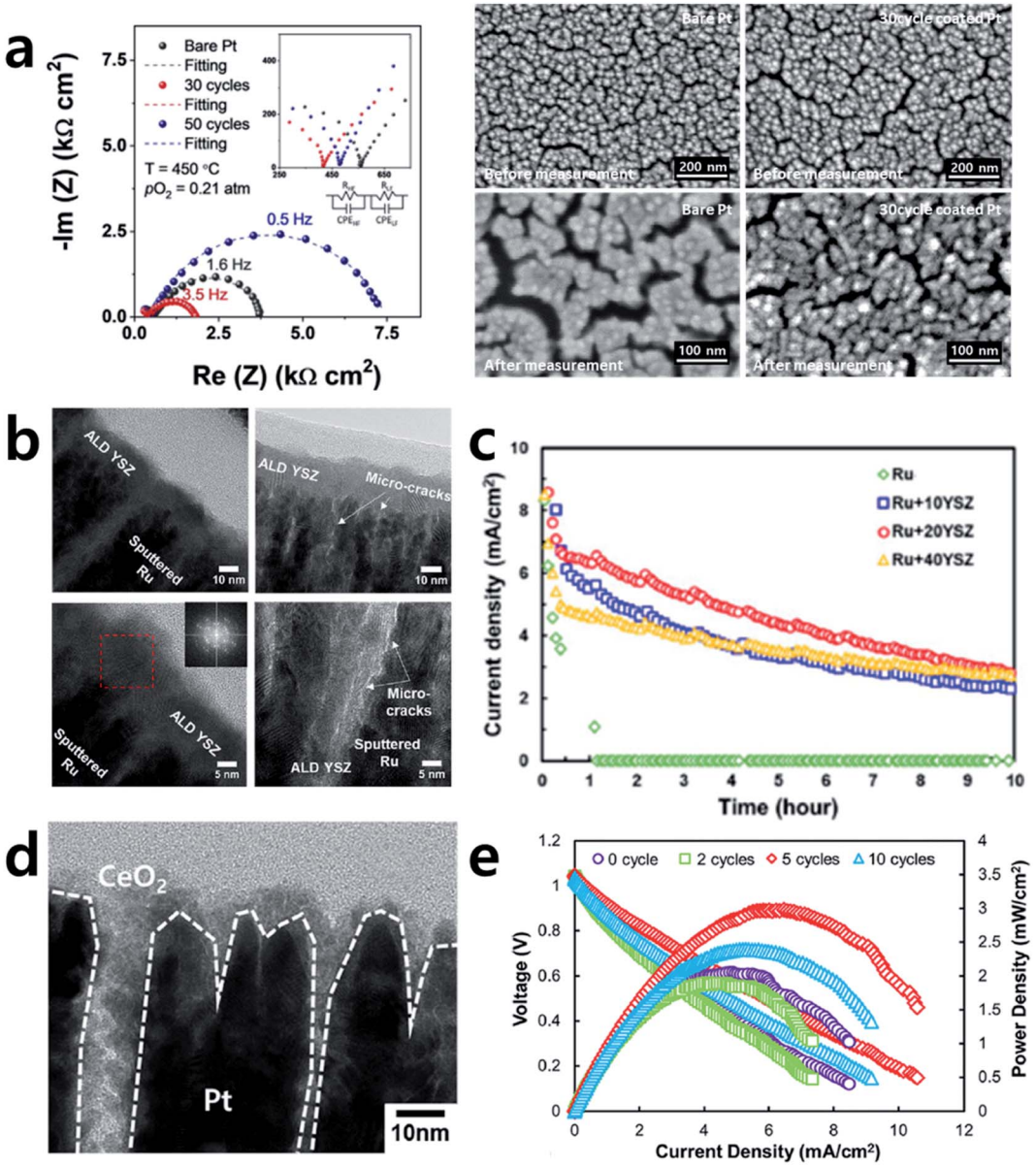

Fig. 6 (a) Typical impedance spectra of bare and Al_2O_3 coated Pt electrodes and SEM images of electrodes with and without Al_2O_3 coating before and after measurement. (b) Cross-sectional TEM images of YSZ coated porous Ru electrodes. (c) Chronoamperometry (at 0.5 V) curves of the cells depending on the thickness of YSZ overcoating. (d) Cross-sectional TEM image of CeO_2 coated porous Pt electrode. (e) Performance comparison of cells with bulk YSZ electrolytes according to the number of CeO_2 ALD cycles. Figures reproduced with permission from ref. 42, 48, and 50. Copyright 2020, Elsevier, and Copyright 2019, American Chemical Society.

electrode was secured with ALD but also a highly active and robust SOFC electrode could be realized even with an electrochemically inert Al_2O_3 coating by sophisticated control of its thickness.

Likewise, there is literature reporting further enhancements of SOFC performance outcomes while ensuring the stability of the metal electrodes by coating functional oxides rather than insulating materials such as Al_2O_3. An *et al.* coated YSZ onto a Ru electrode with ALD and reported its impact on the fuel oxidation reaction at the anode.[42] In their study, 10 nm, 20 nm, and 40 nm layers of YSZ were deposited onto sputtered porous Ru electrodes and their activity and durability with methane fuel were measured. A cross-sectional transmission electron microscopy (TEM) analysis confirmed the uniform YSZ deposition throughout the electrode, with micro-cracks forming on the ALD thin film when exposed to a high temperature, resulting in a fluent fuel supply and TPB expansion (Fig. 6b). It was also found that the cell with an uncoated Ru electrode showed severe performance degradation within a few hours, whereas the cell with the Ru electrode coated with 10 nm of YSZ showed an increased initial power density of 35% with superior their durability as well (Fig. 6c). In addition, the same research team evaluated the ORR properties of Pt electrodes after depositing CeO_2 at various thicknesses using ALD (Fig. 6d), finding that the

Pt–CeO_2 electrode showed higher activity towards the ORR reaction compared to bare Pt and achieving a peak power density of 800 mW cm^{-2} (Fig. 6e), which is the highest value in the literature dealing with nanoporous-substrate-based thin film SOFCs at temperatures below 500 °C, owing to the rapid incorporation of O^{2-} into the Pt–CeO_2 interface.[50]

In parallel with these findings, perovskite oxides (ABO_3) are gaining attention as an electrode material to replace precious metals due to their high electron/oxygen ion conductivity at a high temperature along with their high thermal stability and catalytic activity.[52] However, there is the issue of segregation and the formation of a second phase along with atomic reconstruction on the oxide electrode surface at a high temperature in an oxidizing atmosphere, leading to degradation of the electrode activity.[53–55] For instance, oxides doped with Sr at the A site reportedly show Sr enrichment at the surface under a high temperature and form insulating phases such as SrO on the electrode surface, degrading the performance.[56,57] To deal with this issue, recent studies are being conducted to attain long-term durability by modifying the chemical state of the electrode surface with coating various oxides through dip coating or ALD.[58–62]

Huang *et al.* fabricated a $La_{0.6}Sr_{0.4}CoO_3$ (LSC) thin film electrode with pulsed laser deposition (PLD) and applied a ZrO_2 coating by ALD, after which the surface chemical state change and activity were thoroughly evaluated.[61] As a result, the uncoated LSC electrode showed severe degradation of 4.3 Ω cm^2 h^{-1} at 550 °C; however, the substantially reduced degradation rate of the 0.8 nm ZrO_2-coated LSC was only 0.9 Ω cm^2 h^{-1} (Fig. 7a). *In situ* observations of the chemical state of Sr through ambient pressure X-ray photoelectron spectroscopy (AP-XPS) revealed a significantly reduced atomic fraction of Sr at the surface of the ZrO_2-coated electrode, indicating the successful inhibition Sr segregation *via* the ZrO_2 coating (Fig. 7b). The research team claimed that the ZrO_2 coating on LSC reduces the amount of $V_O^{\cdot\cdot}$ on the LSC surface, in turn reducing the electrostatic interaction with the bulk Sr'_{La} and resulting in the suppression of Sr segregation. In the same vein, Nicholas *et al.* evaluated the activity and surface chemical state changes by depositing various thicknesses of ZrO_2 onto $La_{0.6}Sr_{0.4}Co_{0.8}Fe_{0.2}O_3$ electrodes by ALD.[62] In their study, 5 nm of a ZrO_2 coating on the electrode could successfully mitigate degradation rate with only a 12%/kh degradation rate, whereas an uncoated $La_{0.6}Sr_{0.4}Co_{0.8}Fe_{0.2}O_3$ electrode showed serious degradation of 45%/kh (Fig. 7c). However, unlike in earlier work arguing that the driving force of Sr segregation was restrained, this research team claimed through their XRD analysis (Fig. 7d) that segregated Sr was cleaned up through a reaction with Zr on the surface to form $SrZrO_3$, thereby suppressing the performance degradation. Moreover, they argued that the optimum coating thickness is crucial, as if the deposited layer is too thick, gas channels may not be sufficiently formed in the $SrZrO_3$ layer and thus the activity may decrease accordingly (Fig. 7e).

In these previous examples, successful stabilization was possible because the narrow optimal coating thickness could be explored by enabling nanometer-scale coatings with ALD. However, although there are studies that successfully improved the activity and stability of oxide electrodes through a coating strategy, the exact mechanism of the reaction is still unclear, so even when the same oxide composition is used, their reaction mechanisms are under controversy. In addition, not only the studies that ALD coating is beneficial to the activity and durability of the oxide electrode,[58,59,61,62] but also studies that it has detrimental effect has been reported.[63–65] Therefore, it is essential to conduct further systematical investigations of the surface coating effect on oxide electrodes for the development of highly active/robust oxide electrodes through the ALD coating method.

Lastly, recent studies have reported that not only improving the thermal/chemical stability of the electrode itself but also introducing a robust metal–oxide composite nanocatalyst onto a complex SOFC electrode can effectively realize high-performance SOFC electrodes.[10,66,67] Metal nanocatalysts are applied in various research fields due to their superior catalytic activity.[68] However, their thermal/chemical instability at a high temperature limits their application in devices operated at high temperatures. To overcome this, in the field of thermochemical catalysis, core–shell structures with metal nanoparticles as the core and an oxide with high thermal stability as the shell have been proposed with various synthesis routes, and many successful cases of metal nanocatalyst utilization at a high temperature have been reported.[69] In these cases, the catalytic activity can vary greatly depending on the shell synthesis method and shell morphology, implying that the techniques used to fabricate the sophisticated shell are very important.[69–72] From this perspective, ALD is a very attractive technique to produce the core–shell structure because it uses low deposition temperatures and offers the advantage of uniform and reproducible coatings on complicated structures.[73–75] Recently, Jung *et al.* introduced this strategy in research on SOFCs for the first time, demonstrating that metal–oxide composite nanocatalyst synthesis by ALD can be used to develop a highly active/robust SOFC electrode.[30] The authors successfully developed a highly active/durable electrode by effectively improving the thermal/chemical stability of the Pt nanoparticles on a $La_{0.75}Sr_{0.25}Cr_{0.5}Mn_{0.5}O_3$ (LSCM) electrode using ALD. Fig. 7f shows that Pt nanoparticles 10 nm in size are well dispersed on the LSCM surface by infiltration. Also, through a TEM analysis, uniform ALD coatings of Al_2O_3 on the surface of an LSCM electrode and Pt nanoparticles can be confirmed. This electrode showed nearly 100 times higher electrode activity compared to bare LSCM at 650 °C under CH_4 fuel without degradation for 25 h. Here, they also argued that the optimal coating condition is important by observing the trade-off relationship with the coating thickness. The reason for this is the trade-off relationship between the stability of the Pt nanoparticles and the exposure of the active sites (Fig. 7g). This study not only developed highly active/durable electrodes with methane as fuel but also suggested for the first time that metal nanocatalysts, which were limited in use due to thermal/chemical instability issues, can be applied to high-temperature electrochemical devices by using ALD technology.

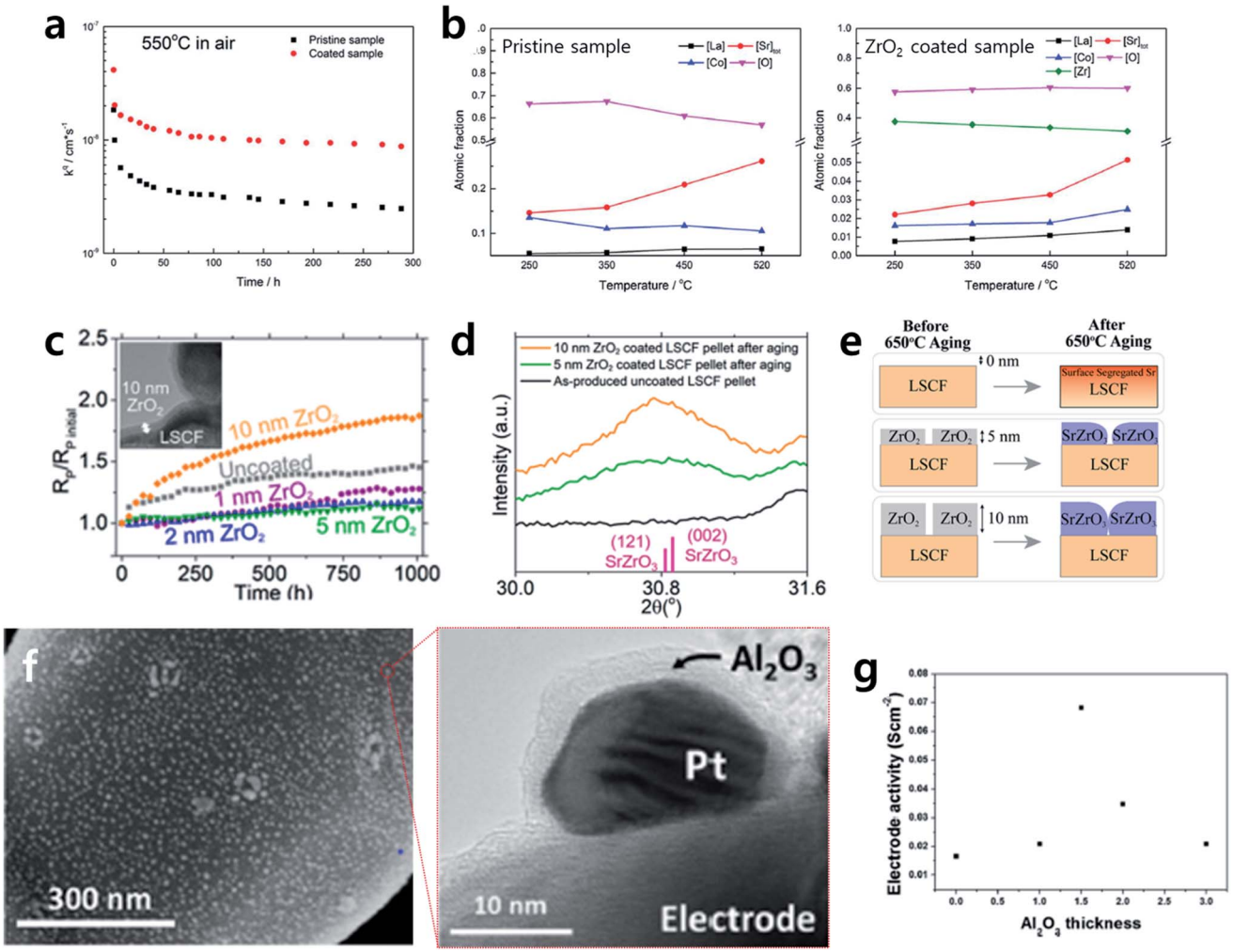

Fig. 7 (a) Time evolution of surface oxygen exchange coefficient of $La_{0.6}Sr_{0.4}CoO_3$ film electrode with and without ZrO_2 ALD coating. (b) Temperature dependent atomic concentrations of pristine and ZrO_2 coated $La_{0.6}Sr_{0.4}CoO_3$ electrode. (c) Aging behavior of normalized polarization resistance depending on the thickness of ZrO_2 ALD coating. (d) X-ray diffraction patterns obtained from pristine $La_{0.6}Sr_{0.4}Co_{0.8}Fe_{0.2}O_3$, 5 nm ZrO_2 coated $La_{0.6}Sr_{0.4}Co_{0.8}Fe_{0.2}O_3$, and 10 nm ZrO_2 coated $La_{0.6}Sr_{0.4}Co_{0.8}Fe_{0.2}O_3$ pellets after aging. (e) Schematics of proposed degradation mechanisms for uncoated and ZrO_2 coated $La_{0.6}Sr_{0.4}Co_{0.8}Fe_{0.2}O_3$. (f) SEM image of Pt nanocatalysts decorated $La_{0.75}Sr_{0.25}Cr_{0.5}Mn_{0.5}O_3$ electrode and TEM image of encapsulated Pt nanocatalysts by Al_2O_3. (g) Electrode activity for CH_4 fuel oxidation of $La_{0.75}Sr_{0.25}Cr_{0.5}Mn_{0.5}O_3$ according to the thickness of Al_2O_3 coating. Figures reproduced with permission from ref. 30, 61, and 62. Copyright 2018, The Royal Society of Chemistry, and Copyright 2020, American Chemical Society.

Studies of the chemical/electrochemical functionalization of electrodes

Along with studies to enhance the stability and activity of SOFC electrodes by improving the thermal/chemical stability through the ALD coating process, research to improve the electrode activity itself by coating functional oxides or metal nanocatalysts onto the surfaces of electrodes is actively underway. Typically, the infiltration method is the most widely used technique for modifying the electrode surface, enabling the introduction of metal/oxide materials with various compositions based on a solution process.[76] However, this requires several infiltration/drying procedures, and it is difficult to control the size distribution and composition of the nanocatalysts reproducibly, which makes this method unsuitable for delicate surface nanoengineering on complicated structures. In contrast, ALD offers the advantage of reproducibly introducing metal nanocatalysts with high uniformity even on complicated structures and easily depositing composite oxides with diverse compositions.[77–86]

Recently, Tsampas reported an example of successful electrode activity enhancement using ALD by uniformly coating Pt nanocatalysts onto an LSCM electrode (Fig. 8a).[85] This research team had developed a technology for introducing 6.5 nm Pt nanoparticles onto a $(La_{0.8}Sr_{0.2})_{0.95}MnO_3/Ce_{0.9}Gd_{0.1}O_{1.95}$ composite electrode in their early work,[87] and using the same technique they succeeded in applying identically sized Pt nanoparticles reproducibly onto a 4 μm-thick LSCM electrode. An electrode with Pt nanoparticle decoration had its electrode resistance reduced to half at 800 °C compared to a bare electrode (Fig. 8b). However, an image analysis of the nanocatalyst

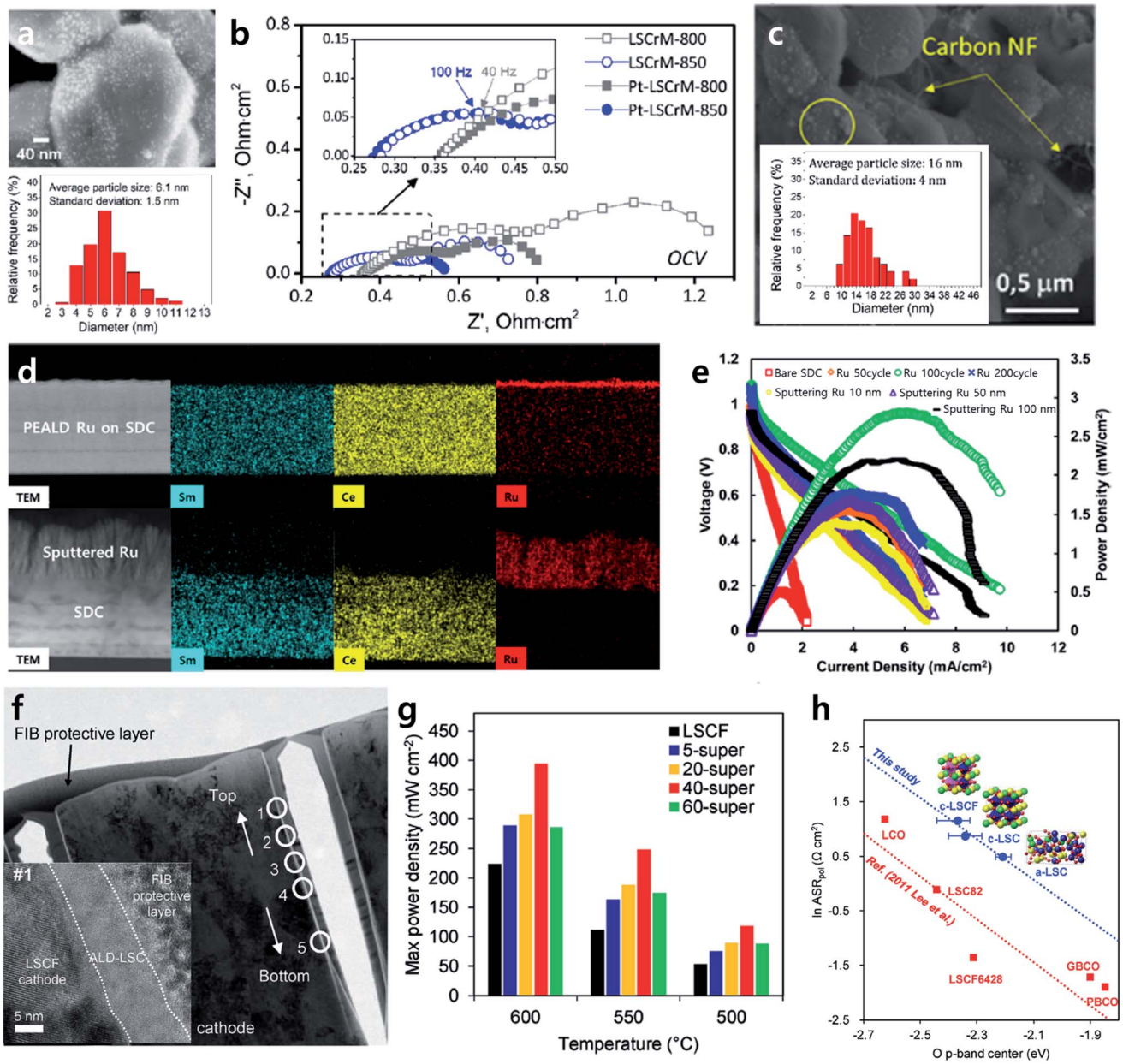

Fig. 8 (a) SEM image of as-deposited Pt nanoparticles on $La_{0.75}Sr_{0.25}Cr_{0.5}Mn_{0.5}O_3$ electrode and their size distribution. (b) Electrochemical performance of $La_{0.75}Sr_{0.25}Cr_{0.5}Mn_{0.5}O_3$ with and without Pt deposition at 800 °C and 850 °C. (c) SEM image of Pt decorated $La_{0.75}Sr_{0.25}Cr_{0.5}Mn_{0.5}O_3$ electrode after operation and size distribution of Pt nanoparticles. (d) Cross-sectional TEM and EDS mapping images of porous Sm doped CeO_2 electrode with Ru coating *via* (above) ALD and (below) sputtering. (e) Comparison of cell performance depending on coating thickness and method. (f) TEM image of the overall microstructure of the $La_{0.6}Sr_{0.4}CoO_3$ coated $La_{0.6}Sr_{0.4}Co_{0.2}Fe_{0.8}O_3$. Inset image is the magnification of region 1. (g) Max power density data of the samples at various temperature depending on the number of ALD super-cycle. (h) The DFT-calculated relative position of the bulk oxygen p-band center to Fermi energy of crystalline $La_{0.6}Sr_{0.4}Co_{0.2}Fe_{0.8}O_3$, crystalline $La_{0.6}Sr_{0.4}CoO_3$, and amorphous $La_{0.6}Sr_{0.4}CoO_3$ with their polarization resistance. Figures reproduced with permission from ref. 81, 83, and 85. Copyright 2020, American Chemical Society, Copyright 2021, American Chemical Society, and Copyright 2018, Wiley.

revealed particle size growth to an average of 18 nm in diameter within only four hours of exposure at 850 °C (Fig. 8c). Although the supported metal nanocatalyst could not maintain its initial microstructure, they found that ALD can decorate small and uniform metal nanocatalysts on various oxide electrodes with good reproducibility. Moreover, this outcome implies that if a metal nanocatalyst stabilizing strategy is realized, it is expected to be a more efficient method for realizing highly active/durable electrodes.

In addition, An *et al.* reported that the plasma-enhanced atomic layer deposition (PEALD) technique can significantly reduce the amount of precious metal usage (2–100 times) by achieving efficient metal catalyst dispersion compared to the conventional sputtering method.[81] PEALD is a type of ALD that

uses plasma as a reactant. It is known to facilitate nucleation in the first few cycles compared to general thermal ALD, providing metal nanocatalysts with high density levels using a very small number of ALD cycles. A TEM analysis showed that Ru deposition by PEALD has high dispersity and a homogeneous distribution throughout the porous SDC electrode, whereas sputtered Ru barely penetrated the complex electrode structure (Fig. 8d). Moreover, when Ru was deposited using PEALD, it showed superior electrode activity at 450 °C in methane fuel, despite the fact that only 5% of the Ru was used compared to the sputtered sample (Fig. 8e). They claimed that they not only maximized the active sites by uniformly coating metal nanocatalysts onto porous electrode but also induced a stronger chemical bond between the Ru particle and the support using PEALD, a CVD process, compared to the physical vapor deposition (PVD) sputtering process. These results suggest a dramatic reduction in precious metal usage for many fields that use metal catalysts as well as SOFC electrodes.

In addition to metal nanocatalyst decoration, Shim *et al.* reported a multicomponent functional oxide deposition technique that greatly improves the electrode ORR activity.[83] The research team successfully deposited a $La_{0.57}Sr_{0.4}CoO_3$ thin film through repeated ALD cycles of $SrO/CoO_x/La_2O_3$. A TEM analysis confirmed the uniform LSC coating onto a porous nanostructured $La_{0.6}Sr_{0.4}Co_{0.2}Fe_{0.8}O_3$ electrode fabricated by PLD. Also, XRD and TEM analyses showed that the LSC film is deposited in the form of an amorphous layer with a certain type of partially crystallized morphology (Fig. 8f). The *I–V* curve showed that the LSC-coated electrode has up to twice the cell performance enhancement at 600 °C compared to a bare electrode, as LSC has higher ORR catalytic activity than LSCF (Fig. 8g). Moreover, the density functional theory (DFT) calculation in this study revealed that amorphous LSC with partial crystallization, prepared through ALD, has higher activity towards the ORR compared to the fully crystallized LSC (Fig. 8h). This study deals with not only an example of successful ORR activity enhancement but also presents the characteristic crystallinity of thin film samples with complex compositions produced by ALD. Hence, there results are meaningful because they suggest that ALD-driven thin film technology is capable of providing new methods for the preparation of high-performance SOFC electrodes.

Studies to facilitate the self-assembly of nanocatalysts

Ex-solution, a nanocatalyst fabrication technology that involves spontaneous phase transformation on the oxide surface under a reducing heat treatment, has been in the spotlight lately in the field of heterogeneous catalysis.[66,67,88,89] The unique property of an ex-solved nanocatalyst is that ex-solved particles are strongly anchored on the support, resulting in high durability at high temperatures compared to nanoparticles prepared by conventional infiltration. Accordingly, this method has brought remarkable progress in the field of SOFCs as well as chemical catalysts.

However, given that ex-solved nanoparticles are generated from the phase transition of a solid solution through a reducing heat treatment, there is a limitation in the amount of ex-solved catalyst. For an accelerated ex-solution process, many studies have attempted to increase the driving force for B site segregation by applying electrical bias or controlling the A site deficiency of the perovskite lattice.[90,91] In line with this effort, Kim *et al.* proposed a topotactic ion exchange strategy to boost the ex-solution process by introducing a guest material that utilized the segregation energy difference.[92] The research team selected $PrBaMn_{1.7}Co_{0.3}O_{5+\delta}$ (PBMCo) including Co with high segregation energy as a support and infiltrated the guest material Fe, known to have much lower segregation energy among transition metals, onto a PBMCo electrode to observe the ex-solution tendency of the system. As shown in Fig. 9a, the number of ex-solved nanoparticles increased as the amount of infiltrated Fe increased. Through DFT calculations, it was confirmed the Co–Fe exchange was thermodynamically more preferred as the surface-incorporated Fe amount increased, which shows that Fe incorporation inside the PBMCo lattice facilitated the ex-solution of Co ions (Fig. 9b). Moreover, a button cell fabricated with a fuel electrode with topotactic ex-solution applied showed performance double that at 800 °C compared to a sample without the introduction of a guest material, demonstrating that guest materials promote ex-solution and at the same time suggesting a new strategy for developing highly active/stable SOFC electrodes. This research team also developed a highly active/stable catalyst for the dry reforming of methane (DRM) by coating Fe_2O_3 onto $La_{0.6}Sr_{0.2}Ti_{0.85}Ni_{0.15}O_{2.95}$ (LSTN) using ALD (Fig. 9c).[93] 10 cycles of ALD coating had a trivial effect on their catalytic activity, but when 20 cycles of Fe_2O_3 coating were applied, a 64% increase in the methane conversion ratio and a 40% reduction in the activation energy were achieved compared to a bare LSTN sample (Fig. 9d). Furthermore, the catalyst showed steady methane conversion for more than 400 hours of operation at 700 °C without any performance degradation. The research team claimed that a superior catalyst could be developed because uniform topotactic ex-solution was achieved with an ALD coating *via* the homogeneous deposition of a guest material throughout the catalyst surface, and optimal loading was obtained through precise thickness control. These results represent the first report of the design of the self-assembly of nanocatalysts using ALD. This implies that ALD technology can be applied to various high-temperature applications of SOFCs, protonic ceramic fuel cells (PCFC), and to the catalysis field to fabricate a highly active/stable catalyst by promoting the uniform self-assembly of nanoparticles on the surface.

Concluding remarks and outlook

This review has shown that ALD technology is actively being applied currently in the SOFC field, resolving many issues and pioneering this new research field. ALD, with the advantage of high step coverage and scalability, is already widely used on the production lines of the semiconductor industry and is further expanding its application to other fields in need of nanoscale engineering. In the SOFC field, it has greatly contributed to the fabrication of thin and dense electrolytes for intermediate SOFC

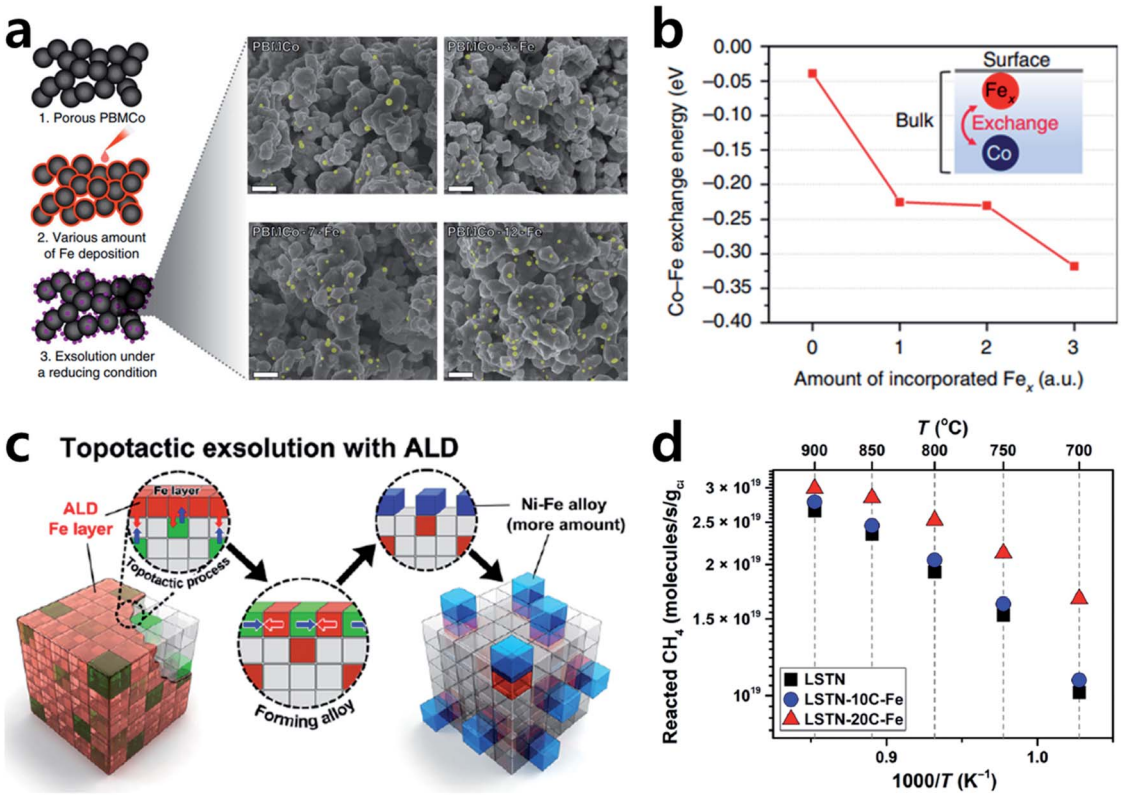

Fig. 9 (a) SEM images of $Pr_{0.5}Ba_{0.5}Mn_{0.85}Co_{0.15}O_3$, $Pr_{0.5}Ba_{0.5}Mn_{0.85}Co_{0.15}O_3$ with 3 wt% infiltration of Fe, $Pr_{0.5}Ba_{0.5}Mn_{0.85}Co_{0.15}O_3$ with 7 wt% infiltration of Fe, and $Pr_{0.5}Ba_{0.5}Mn_{0.85}Co_{0.15}O_3$ with 12 wt% infiltration of Fe after exsolution. (b) Calculated energetics for the Co–Fe$_x$ exchange depending on the arbitrary Fe concentration. (c) Schematics of topotactic exsolution *via* ALD. (d) Reacted methane during the dry reforming of methane for $La_{0.6}Sr_{0.2}Ti_{0.85}Ni_{0.15}O_3$, $La_{0.6}Sr_{0.2}Ti_{0.85}Ni_{0.15}O_3$ with 10 cycles of Fe_2O_3, and $La_{0.6}Sr_{0.2}Ti_{0.85}Ni_{0.15}O_3$ with 20 cycles of Fe_2O_3. Figures reproduced with permission from ref. 92, and 93. Copyright 2019, Springer Nature, Copyright 2020, American Association for the Advancement of Science.

development and to the enhancement of performance outcomes by modifying electrode/electrolyte interfaces with different oxide coating. Specifically, the introduction of ALD with high step coverage has enabled precise and uniform nanoscale engineering on structurally complex surfaces of SOFC electrodes, suggesting a novel high-performance/durable SOFC electrode fabrication strategy through surface chemistry engineering and metal/oxide composite nanocatalyst synthesis. However, material studies of the effect of oxide coatings with more diverse compositions on SOFC electrodes are still lacking, and further research is required to determine the exact mechanism of how the ALD coating affects the reactivity and durability of SOFC electrodes. For example, Vohs *et al.* evaluated the ORR reactivity of oxide electrode, $(La_{0.8}Sr_{0.2})MO_3$ (M = Fe, Mn, and Co), after depositing variety of materials such as SrO, La_2O_3, Pr_2O_3 of various thicknesses using ALD.[94] Interestingly, the research team observed the huge reduction in polarization resistance for ORR of more than 40% when they deposited SrO and La_2O_3 as a monolayer, which are known as inert and insulating material for electrochemical reaction. This is the result of breaking the conventional belief for a long time that SrO is an electrochemically detrimental material, through a very precise thickness control by ALD. Therefore, if additional research using ALD is conducted on more diverse material combinations, it will serve as a research strategy to explore new material properties. Furthermore, in the field of supported catalysts, Gorte *et al.* reported that coating perovskite oxide on the catalyst support can be a strategy to dramatically stabilize the supported catalysts at high temperature.[95] The research team observed that supported Pt catalysts on $LaFeO_3$ coated $MgAl_2O_4$ support oxide are epitaxially aligned with respect to the $LaFeO_3$ and the consequent strong metal–support interaction between Pt and $LaFeO_3$ stabilizes Pt catalyst at high temperature redox cycling. This observation is a new discovery in the heterogeneous catalysts field, and thus the noble research field to design a highly durable and active metal/ceramic nanocomposite SOFC can be pioneered by surface engineering applied between the nanocatalysts and the electrode surface as well as fabricating the core–shell structure through ALD.

Using the examples probed in this review as a guide, more active applications of ALD technology in the field of SOFC and a new leap towards the realization of highly active/durable electrolytes and electrodes can be expected. Furthermore, we hope that the new achievements obtained from ALD studies in the SOFC field can provide new insights into

various high-temperature applications requiring nanoscale engineering.

Conflicts of interest

There are no conflicts to declare.

Acknowledgements

This work was supported by the Korea Institute of Energy Technology Evaluation and Planning (KETEP) and the Ministry of Trade, Industry & Energy (MOTIE) of the Republic of Korea (No. 20194030202360) and the research fund of Hanbat National University in 2021.

References

1 M. A. Azizi and J. Brouwer, *Appl. Energy*, 2018, **215**, 237–289.
2 S. McIntosh and R. J. Gorte, *Chem. Rev.*, 2004, **104**, 4845–4865.
3 N. Q. Minh, *J. Am. Ceram. Soc.*, 1993, **76**, 563–588.
4 Z. P. Shao and S. M. Haile, *Nature*, 2004, **431**, 170–173.
5 E. D. Wachsman and K. T. Lee, *Science*, 2011, **334**, 935–939.
6 Z. Gao, L. V. Mogni, E. C. Miller, J. G. Railsback and S. A. Barnett, *Energy Environ. Sci.*, 2016, **9**, 1602–1644.
7 J. T. S. Irvine, D. Neagu, M. C. Verbraeken, C. Chatzichristodoulou, C. Graves and M. B. Mogensen, *Nat. Energy*, 2016, **1**, 15014–15026.
8 J. An, J. H. Shim, Y. B. Kim, J. S. Park, W. Lee, T. M. Gur and F. B. Prinz, *MRS Bull.*, 2014, **39**, 798–804.
9 A. Evans, A. Bieberle-Hutter, J. L. M. Rupp and L. J. Gauckler, *J. Power Sources*, 2009, **194**, 119–129.
10 P. A. Connor, X. L. Yue, C. D. Savaniu, R. Price, G. Triantafyllou, M. Cassidy, G. Kerherve, D. J. Payne, R. C. Maher, L. F. Cohen, R. I. Tomov, B. A. Glowacki, R. V. Kumar and J. T. S. Irvine, *Adv. Energy Mater.*, 2018, **8**, 1800120.
11 S. M. George, *Chem. Rev.*, 2010, **110**, 111–131.
12 B. C. Mallick, C. T. Hsieh, K. M. Yin, Y. A. Gandomi and K. T. Huang, *ECS J. Solid State Sci. Technol.*, 2019, **8**, N55–N78.
13 X. B. Meng, X. W. Wang, D. S. Geng, C. Ozgit-Akgun, N. Schneider and J. W. Elam, *Mater. Horiz.*, 2017, **4**, 133–154.
14 J. J. Pyeon, I. H. Baek, Y. G. Song, G. S. Kim, A. J. Cho, G. Y. Lee, J. H. Han, T. M. Chung, C. S. Hwang, C. Y. Kang and S. K. Kim, *J. Mater. Chem. C*, 2020, **8**, 11874–11881.
15 O. Tiurin and Y. Ein-Eli, *Adv. Mater. Interfaces*, 2019, **6**, 1901455.
16 D. Yu, Y. Q. Yang, Z. Chen, Y. Tao and Y. F. Liu, *Opt. Commun.*, 2016, **362**, 43–49.
17 V. Zardetto, B. L. Williams, A. Perrotta, F. Di Giacomo, M. A. Verheijen, R. Andriessen, W. M. M. Kessels and M. Creatore, *Sustainable Energy Fuels*, 2017, **1**, 30–55.
18 J. H. Kim, T. J. Park, S. K. Kim, D. Y. Cho, H. S. Jung, S. Y. Lee and C. S. Hwang, *Appl. Surf. Sci.*, 2014, **292**, 852–856.
19 M. Ylilammi, *Thin Solid Films*, 1996, **279**, 124–130.
20 J. H. Kim, T. J. Park, M. Cho, J. H. Jang, M. Seo, K. D. Na, C. S. Hwang and J. Y. Won, *J. Electrochem. Soc.*, 2009, **156**, G48–G52.
21 J. M. Lee, J. Lee, J. W. Han, H. Park, S. Kyung, I. Kim, J. M. Lee, T. J. Park and W. H. Kim, *Appl. Surf. Sci.*, 2021, **539**, 148247–148253.
22 A. L. Johnson and J. D. Parish, *Organometallic Chemistry*, 2019, vol. 42, pp. 1–53.
23 H. H. Sonsteby, A. Yanguas-Gil and J. W. Elam, *J. Vac. Sci. Technol., A*, 2020, **38**, 020804.
24 R. W. Johnson, A. Hultqvist and S. F. Bent, *Mater. Today*, 2014, **17**, 236–246.
25 S. K. Kim, K. M. Kim, D. S. Jeong, W. Jeon, K. J. Yoon and C. S. Hwang, *J. Mater. Res.*, 2013, **28**, 313–325.
26 H. K. Kim, H. S. Jung, J. H. Jang, J. Park, T. J. Park, S. H. Lee and C. S. Hwang, *J. Appl. Phys.*, 2011, **110**.
27 T. J. Park, J. H. Kim, J. H. Jang, C. K. Lee, K. D. Na, S. Y. Lee, H. S. Jung, M. Kim, S. Han and C. S. Hwang, *Chem. Mater.*, 2010, **22**, 4175–4184.
28 J. Li, Y. H. Zhou, D. Y. Zhong, C. X. Huang, J. Huang and J. H. Zhang, *Electron. Mater. Lett.*, 2018, **14**, 669–677.
29 S. Jo, B. Sharma, D. H. Park and J. H. Myung, *J. Korean Ceram. Soc.*, 2020, **57**, 135–151.
30 J. Seo, N. Tsvetkov, S. J. Jeong, Y. Yoo, S. Ji, J. H. Kim, J. K. Kang and W. Jung, *ACS Appl. Mater. Interfaces*, 2020, **12**, 4405–4413.
31 Y. M. Lyu, F. F. Wang, D. B. Wang and Z. L. Jin, *Mater. Technol.*, 2020, **35**, 212–227.
32 W. Yu, Y. Lim, S. Lee, A. Pandiyan, G. Y. Cho and S. W. Cha, *J. Mater. Chem. A*, 2020, **8**, 21668–21679.
33 Z. Zakaria, Z. A. Mat, S. H. Abu Hassan and Y. B. Kar, *Int. J. Energy Res.*, 2020, **44**, 594–611.
34 G. Y. Cho, Y. H. Lee, W. Yu, J. An and S. W. Cha, *Energy*, 2019, **173**, 436–442.
35 S. Ji, *Int. J. Precis. Eng. Manuf.*, 2020, **21**, 1085–1090.
36 S. Oh, J. Park, J. W. Shin, B. C. Yang, J. M. Zhang, D. Y. Jang and J. An, *J. Mater. Chem. A*, 2018, **6**, 7401–7408.
37 J. H. Shim, C. C. Chao, H. Huang and F. B. Prinz, *Chem. Mater.*, 2007, **19**, 3850–3854.
38 B. C. Yang, D. Go, S. Oh, J. W. Shin, H. J. Kim and J. An, *Appl. Surf. Sci.*, 2019, **473**, 102–106.
39 H. Yang, H. Lee, Y. Lim and Y. B. Kim, *J. Am. Ceram. Soc.*, 2021, **104**, 86–95.
40 J. G. Yu, B. C. Yang, J. W. Shin, S. Lee, S. Oh, J. H. Choi, J. Jeong, W. Noh and J. An, *Ceram. Int.*, 2019, **45**, 3811–3815.
41 Y. Choi, S. K. Cha, H. Ha, S. Lee, H. K. Seo, J. Y. Lee, H. Y. Kim, S. O. Kim and W. Jung, *Nat. Nanotechnol.*, 2019, **14**, 245–251.
42 D. Go, B. C. Yang, J. W. Shin, H. J. Kim, S. Lee, S. Kye, S. Kim and J. An, *Ceram. Int.*, 2020, **46**, 1705–1710.
43 S. Ji and W. H. Tanveer, *Appl. Surf. Sci.*, 2020, **514**, 145931–145935.
44 H. Kim, H. G. Seo, Y. Choi, D. K. Lim and W. Jung, *J. Mater. Chem. A*, 2020, **8**, 14491–14497.
45 J. Lim, J. W. Shim, D. J. Kim, J. S. Park, J. Koo and J. H. Shim, *J. Power Sources*, 2021, **498**, 229923–229930.

46 J. Oh, G. Seo, J. Kim, S. Bae, J. W. Park and J. H. Hwang, *Coatings*, 2021, **11**, 362–374.
47 B. K. Park, H. G. Seo, W. Jung and J. W. Lee, *Ceram. Int.*, 2018, **44**, 18727–18735.
48 H. G. Seo, S. Ji, J. Seo, S. Kim, B. Koo, Y. Choi, H. Kim, J. H. Kim, T. S. Kim and W. Jung, *J. Alloys Compd.*, 2020, **835**, 155347–155353.
49 J. W. Shin, S. Oh, S. Lee, D. Go, J. Park, H. J. Kim, B. C. Yang, G. Y. Cho and J. An, *Int. J. Hydrogen Energy*, 2021, **46**, 20087–20092.
50 J. W. Shin, S. Oh, S. Lee, J. G. Yu, J. Park, D. Go, B. C. Yang, H. J. Kim and J. An, *ACS Appl. Mater. Interfaces*, 2019, **11**, 46651–46657.
51 M. Benamira, L. Niinisto, A. Ringuede and M. Cassir, *Mater. Chem. Phys.*, 2020, **241**, 122386–122393.
52 Y. B. Chen, W. Zhou, D. Ding, M. L. Liu, F. Ciucci, M. Tade and Z. P. Shao, *Adv. Energy Mater.*, 2015, **5**, 1500537–1500570.
53 B. Koo, K. Kim, J. K. Kim, H. Kwon, J. W. Han and W. Jung, *Joule*, 2018, **2**, 1476–1499.
54 B. Koo, H. Kwon, Y. Kim, H. G. Seo, J. W. Han and W. Jung, *Energy Environ. Sci.*, 2018, **11**, 71–77.
55 B. Koo, J. Seo, J. K. Kim and W. Jung, *J. Mater. Chem. A*, 2020, **8**, 13763–13769.
56 Z. H. Cai, M. Kubicek, J. Fleig and B. Yildiz, *Chem. Mater.*, 2012, **24**, 1116–1127.
57 W. Jung and H. L. Tuller, *Energy Environ. Sci.*, 2012, **5**, 5370–5378.
58 Y. H. Gong, D. Palacio, X. Y. Song, R. L. Patel, X. H. Liang, X. Zhao, J. B. Goodenough and K. Huang, *Nano Lett.*, 2013, **13**, 4340–4345.
59 Y. H. Gong, R. L. Patel, X. H. Liang, D. Palacio, X. Y. Song, J. B. Goodenough and K. Huang, *Chem. Mater.*, 2013, **25**, 4224–4231.
60 N. Tsvetkov, Q. Y. Lu, L. X. Sun, E. J. Crumlin and B. Yildiz, *Nat. Mater.*, 2016, **15**, 1010–1016.
61 Y. T. Wen, T. R. Yang, D. Lee, H. N. Lee, E. J. Crumlin and K. Huang, *J. Mater. Chem. A*, 2018, **6**, 24378–24388.
62 Y. B. Zhang, Y. T. Wen, K. Huang and J. D. Nicholas, *ACS Appl. Energy Mater.*, 2020, **3**, 4057–4067.
63 E. H. Kim, H. J. Jung, K. S. An, J. Y. Park, J. Lee, I. D. Hwang, J. Y. Kim, M. J. Lee, Y. Kwon and J. H. Hwang, *Ceram. Int.*, 2014, **40**, 7817–7822.
64 M. Rahmanipour, Y. Cheng, T. M. Onn, A. Donazzi, J. M. Vohs and R. J. Gorte, *J. Electrochem. Soc.*, 2017, **164**, F879–F884.
65 A. S. Yu, R. Kungas, J. M. Vohs and R. J. Gorte, *J. Electrochem. Soc.*, 2013, **160**, F1225–F1231.
66 T. Y. Cao, O. Kwon, R. J. Gorte and J. M. Vohs, *Nanomaterials*, 2020, **10**, 2445–2467.
67 J. H. Kim, J. K. Kim, J. Liu, A. Curcio, J. S. Jang, I. D. Kim, F. Ciucci and W. Jung, *ACS Nano*, 2021, **15**, 81–110.
68 R. J. White, R. Luque, V. L. Budarin, J. H. Clark and D. J. Macquarrie, *Chem. Soc. Rev.*, 2009, **38**, 481–494.
69 M. Cargnello, P. Fornasiero and R. J. Gorte, *Catal. Lett.*, 2012, **142**, 1043–1048.
70 S. Kim, S. Lee and W. Jung, *ChemCatChem*, 2019, **11**, 4653–4659.
71 S. Lee, J. Seo and W. Jung, *Nanoscale*, 2016, **8**, 10219–10228.
72 M. Monai, T. Montini, C. Chen, E. Fonda, R. J. Gorte and P. Fornasiero, *ChemCatChem*, 2015, **7**, 2038–2046.
73 B. J. O'Neill, D. H. K. Jackson, J. Lee, C. Canlas, P. C. Stair, C. L. Marshall, J. W. Elam, T. F. Kuech, J. A. Dumesic and G. W. Huber, *ACS Catal.*, 2015, **5**, 1804–1825.
74 J. A. Singh, N. Y. Yang and S. F. Bent, in *Annual Review of Chemical and Biomolecular Engineering*, ed. J. M. Prausnitz, 2017, vol. 8, pp. 41–62.
75 B. Zhang and Y. Qin, *ACS Catal.*, 2018, **8**, 10064–10081.
76 J. M. Vohs and R. J. Gorte, *Adv. Mater.*, 2009, **21**, 943–956.
77 Y. Chen, K. Gerdes, S. A. P. Navia, L. Liang, A. Hinerman and X. Y. Song, *Nano Lett.*, 2019, **19**, 8767–8773.
78 Y. Chen, S. A. Paredes-Navia, C. O. Romo-De-La-Cruz, L. Liang, A. Fernandes, A. Hinerman, J. Prucz, M. Williams and X. Y. Song, *J. Power Sources*, 2021, **499**, 229854–229861.
79 E. Dogdibegovic, R. F. Wang, G. Y. Lau, A. Karimaghaloo, M. H. Lee and M. C. Tucker, *J. Power Sources*, 2019, **437**, 226935–226943.
80 D. Y. Jang, J. Koo, H. R. Choi, J. W. Kim, H. J. Jeong, F. B. Prinz and J. H. Shim, *ACS Sustainable Chem. Eng.*, 2020, **8**, 10529–10535.
81 S. Kye, H. J. Kim, D. Go, B. C. Yang, J. W. Shin, S. Lee and J. An, *ACS Catal.*, 2021, **11**, 3523–3529.
82 C. Lin, A. C. Foucher, Y. C. Ji, E. A. Stach and R. J. Gorte, *J. Mater. Chem. A*, 2020, **8**, 16973–16984.
83 H. J. Choi, K. Bae, S. Grieshammer, G. D. Han, S. W. Park, J. W. Kim, D. Y. Jang, J. Koo, J. Son, M. Martin and J. H. Shim, *Adv. Energy Mater.*, 2018, **8**, 1802506.
84 J. M. Paige, D. Vu, T. Y. Cao, S. McIntosh, R. J. Gorte and J. M. Vohs, *J. Electrochem. Soc.*, 2021, **168**, 084502–084508.
85 A. Pandiyan, V. Di Palma, V. Kyriakou, W. M. M. Kessels, M. Creatore, M. C. M. van de Sanden and M. N. Tsampas, *ACS Sustainable Chem. Eng.*, 2020, **8**, 12646–12654.
86 J. F. Roeder, M. Golalikhani, A. F. Zeberoff, P. C. Van Buskirk, A. Torabi, J. M. Barton, C. M. Willman, H. Ghezel-Ayagh, Y. Wen and K. Huang, *ECS Trans.*, 2017, **78**, 935–942.
87 Y. Hajar, V. Di Palma, V. Kyriakou, M. A. Verheijen, E. A. Baranova, P. Vernoux, W. M. M. Kessels, M. Creatore, M. C. M. van de Sanden and M. N. Tsampas, *Electrochem. Commun.*, 2017, **84**, 40–44.
88 J. H. Kim, J. K. Kim, H. G. Seo, D. K. Lim, S. J. Jeong, J. Seo, J. Kim and W. Jung, *Adv. Funct. Mater.*, 2020, **30**, 2001326–2001334.
89 J. K. Kim, Y. R. Jo, S. Kim, B. Koo, J. H. Kim, B. J. Kim and W. Jung, *ACS Appl. Mater. Interfaces*, 2020, **12**, 24039–24047.
90 J. H. Myung, D. Neagu, D. N. Miller and J. T. S. Irvine, *Nature*, 2016, **537**, 528–531.
91 D. Neagu, G. Tsekouras, D. N. Miller, H. Menard and J. T. S. Irvine, *Nat. Chem.*, 2013, **5**, 916–923.
92 S. Joo, O. Kwon, K. Kim, S. Kim, H. Kim, J. Shin, H. Y. Jeong, S. Sengodan, J. W. Han and G. Kim, *Nat. Commun.*, 2019, **10**, 697–705.

93 S. Joo, A. Seong, O. Kwon, K. Kim, J. H. Lee, R. J. Gorte, J. M. Vohs, J. W. Han and G. Kim, *Sci. Adv.*, 2020, **6**, eabb1573–eabb1580.
94 Y. Cheng, A. S. Raman, J. Paige, L. Zhang, D. Y. Sun, M. U. Chen, A. Vojvodic, R. J. Gorte and J. M. Vohs, *J. Phys. Chem. Lett.*, 2019, **10**, 4082–4088.
95 X. Y. Mao, A. C. Foucher, T. Montini, E. A. Stach, P. Fornasiero and R. J. Gorte, *J. Am. Chem. Soc.*, 2020, **142**, 10373–10382.